Fine structure in the intrinsic absorption edge of TiO_2

J. Pascual, J. Camassel, and H. Mathieu
Centre d'Etudes d'Electronique des Solides, Université des Sciences et Techniques du Languedoc, 34060-Montpellier-Cedex, France*
(Received 21 June 1977)

The polarization-dependent absorption spectra and wavelength-modulated absorption spectra of TiO_2 have been measured under very-high-resolution conditions between 1.6 and 300°K. For the first time the fine structure of the fundamental absorption edge is resolved and a detailed investigation is presented. We find an indirect allowed transition $\Sigma_{4v} \rightarrow \Gamma_{1c}$, characterized by a small doublet (3.061-3.065 eV at 1.6°K) which constitutes the fundamental transition in polarization $\vec{E}$ parallel to $\vec{C}$. In polarization perpendicular to $\vec{C}$, we find the same indirect transition plus a new forbidden direct transition $\Gamma_{3v} \rightarrow \Gamma_{1c}$ which appears at slightly lower energy (3.031 eV at 1.6°K). The fine structure of the forbidden exciton is resolved and the ionization energy is 4 meV.

I. INTRODUCTION

TiO_2 (rutile) is a wide-band-gap semiconductor which has promising applications in economical photolysis of water. It has also applications related with the large value of its dielectric constant and the large dielectric anisotropy. The electronic structure of rutile is usually described in terms of an ionic model based on the ions Ti^{4+} and O^{2-}. The valence band is mainly built of oxygen p states and the conduction band of empty titanium d states. The crystal structure is tetragonal, D_{4h}^{14}, with 6 ions per primitive unit cell.

In the energy range 4–10 eV, room-temperature reflectivity[1] and electroreflectance studies[2] have been reported in polarization parallel and perpendicular to $\vec{C}$. Both sets of data are in good agreement and account well for the dielectric anisotropy. In polarization $\vec{E} \| \vec{C}$, the imaginary part of the dielectric constant exhibits only one main absorption band centered around 4.3 eV at room temperature which originates from the p_z orbitals of oxygen and determines the long-wavelength dispersion. In polarization $\vec{E} \perp \vec{C}$, the crystal-field splitting of the p_x-p_y bands gives two maxima. The center of gravity of the doublet appears at ~4.5 eV and is in excellent agreement with the refractive-index data.[1,3] Most recently, a band-structure calculation for TiO_2 has been published,[4] and a comparison of calculated interband energies with optical-critical-point values has been attempted. The agreement is found satisfactory, and both calculation and experiment suggest that the first direct allowed transition in TiO_2 falls around 3.5 eV.

However, from absorption data and photoconductivity studies,[5] the fundamental absorption edge is found to be lower (about 3.05 eV at low temperature) and probably indirect. Up to now, no fine structure or identification of the possible phonons involved in the fundamental absorption mechanism has been reported. At liquid-nitrogen temperature, unsuccessful attempts have been made. Both electroabsorption (EA) and electroreflectance (ER) studies have been published.[6,7] They suggest a complex participation of indirect allowed and direct forbidden transitions without a definite assignment.

In this paper, we report absorption spectra and wavelength-modulated absorption spectra obtained for TiO_2 under very-high-resolution conditions. Working at temperatures ranging between 1.6 °K and 300 °K, we have resolved the fine structure of the fundamental absorption edge for the first time. We find an indirect transition $\Sigma_{4v} \rightarrow \Gamma_{1c}$, characterized by a small doubled (3.061–3.065 eV at 1.6 °K), which constitutes the fundamental transition in polarization parallel to $\vec{C}$. From a comparison of the phonon energies with recent neutron-diffraction data, we give a localization of the valence band extrema in k space $[0.2(2\pi/a)(1,1,0)]$. In polarization perpendicular to $\vec{C}$, we find the same indirect absorption edge plus a new forbidden direct transition which appears at slightly lower energy (3.031 eV at 1.6 °K). We show that a weak quadrupolar interaction slightly allows 1s-exciton creation.

II. EXPERIMENTAL DETAILS

After a careful x-ray orientation, the synthetic TiO_2 crystals used in this work were cut and polished in a standard manner. Our samples had thicknesses of 23, 90, 350, and 1830 microns but most data were recorded on the 23-μ-thick sample. With the use of uv polaroid sheets, the polarization ratio of the incident light was checked over the wavelength range of investigation. It was found better than 98%. The alignment of the po-

larization angle with respect to the C axis was better than 1°.

We have used a high-resolution, Jobin-Yvon THR 1500 spectrometer, which allows a practical resolving power better than 150 000. The modulation spectra $\Delta T/T$ were recorded using a slight modulation of the output mirror in front of the exit slit. The driving frequency was 350 Hz and both dc (transmission) and ac (first-order derivative of the transmission) detection techniques were used.[8] The ratio of both signals was done electronically.

During standard absorption measurements, the energy dependence of the transmitted light was carefully checked well below the threshold. It closely followed the energy dependence of the incident intensity I_0 and multiple internal reflexion effects were found negligible. The absorption coefficient was therefore simply calculated assuming $\alpha = 0$ in the range of constant I_T/I_0.

Two different cryogenic systems were used. A pumped helium bath for measurements at 1.6 °K and a variable temperature cryostat for measurements between 10 and 300 °K. In this case, the temperature was measured by means of carbon and/or platinum resistances.

III. RESULTS

In Figs. 1 and 2 we give some representative absorption curves for a series of temperatures ranging from 1.6 to 260 °K. Figure 1 displays the data for polarization $\vec{E} \| \vec{C}$ and Fig. 2 for polarization $\vec{E} \perp \vec{C}$.

The set of curves in Fig 1 ($\vec{E} \| \vec{C}$) shows the general step structure characteristic of the intrinsic

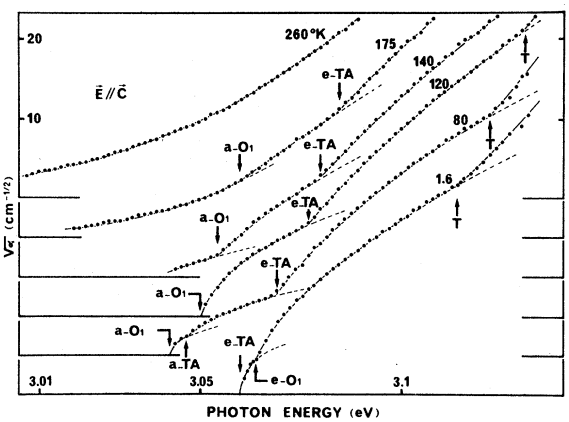

FIG. 1. Typical absorption spectrum for TiO_2 in polarization parallel to $\vec{C}$ at different temperatures. Most data were obtained on a 23-μ-thick sample. For clarity, we have displayed the different curves with a vertical shift of 5 $cm^{-1/2}$.

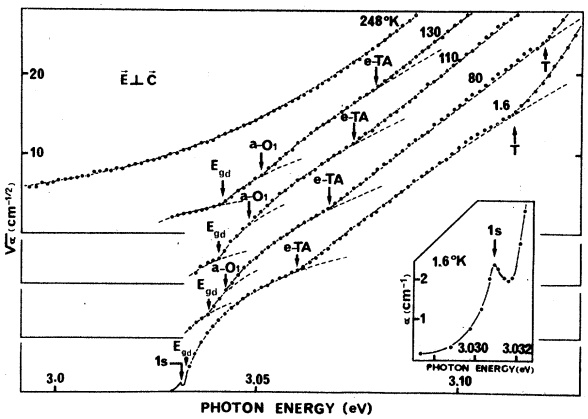

FIG. 2. Same as Fig. 1, but in polarization perpendicular to $\vec{C}$. The inset shows on an expended scale the 1s forbidden exciton of TiO_2.

absorption edge for crystals with an indirect energy gap E_{gi}. We label the different thresholds according to the phonon mode which assists the electronic transition (see Sec. IV A). The prefix denotes whether the phonon is emitted (e) or absorbed (a). As usual, we find at low temperature (1.6 °K) only components corresponding with an emission of phonons. We resolve three components, each characterized by a well-defined knee. The two first, e-TA and e-O_1, are within 4 meV. Increasing the temperature, the replica corresponding with absorbed phonons appear on the low-energy side of the curves. The relative strength of these phonon-absorption components increases continuously with temperature and smears out the entire spectrum at about 260 °K. Also, we note that the whole absorption spectrum is translated to higher energies as the temperature increases, showing a positive temperature dependence of the energy gap E_{gi}.

In Fig. 2 we show the absorption curves for $\vec{E} \perp \vec{C}$. We find the two different sets of structures listed in Table I. Most of them where previously seen in configuration $\vec{E} \| \vec{C}$ and are associated with the indirect gap. However, at lower energy, an additional threshold E_{gd} is now resolved and, at very low temperature (see insert in Fig. 2), a very sharp excitonic structure (1s) also appears. Increasing the temperature, E_{gd} shifts also to higher energies but even on our thickest sample (~1 cm) we have been unable to find any phonon replica of this structure. This absorption does not present the behavior of an indirect phonon-assisted transition and will be discussed at length in Sec. IV B.

Figure 3 shows the temperature dependence of the different thresholds. The indirect energy gap E_{gi}, found in both parallel and perpendicular to $\vec{C}$ configurations, is shown as the central dashed

TABLE I. Energy threshold for TiO_2 at 1.6 °K, 80 °K, and extrapolated values at room temperature.

TiO_2		Direct-gap structures 1s	Direct-gap structures E_{gd}	Indirect-gap structures a-O_1	Indirect-gap structures a-TA	Indirect-gap structures E_{gi}	Indirect-gap structures e-TA	Indirect-gap structures e-O_1	High-energy threshold T
1.6 °K	$\vec{E}\parallel\vec{C}$	Forbidden	Forbidden	···	···	3049	3060	3064	3115
	$\vec{E}\perp\vec{C}$	3031	3033	···	···	3049	3060	3064	3114
80 °K	$\vec{E}\parallel\vec{C}$	Forbidden	Forbidden	3042	3046	3057	3068	···	3122
	$\vec{E}\perp\vec{C}$	···	3038	3042	···	3057	3068	···	3121
300 °K (extrapolation values)		···	3062	···	···	3101	···	···	3166

line. It is given as the arithmetic mean of the threshold energies of the pair of absorption components corresponding to the same phonon energy. Up to about 35 °K, we observe clearly the two emitted phonons e-O_1 and e-TA. However, above 40 °K, we can only resolve the low-energy component e-TA. Similarly, for the two absorbed phonons, we find both a-O_1 and a-TA up to 100 °K, but above this temperature only the low-energy component is resolved. The variation of E_{gi} versus temperature is linear above ~60 °K with a temperature coefficient

$$\frac{dE_{gi}}{dT} = 1.98\times10^{-4}\ \text{eV/°K}.$$

At room temperature, we find by extrapolation a value $E_{gi} = 3.101$ eV. Let us remark that (i) the T structure (3114 meV at 1.6 °K) closely parallels the temperature dependence of the indirect gap E_{gi}. It corresponds also to an indirect transition and will be discussed in Sec. IV C; (ii) the direct gap E_{gd} and the sharp 1s structures show a smaller temperature dependence,

$$\frac{dE_{gd}}{dT} = 1.77\times10^{-4}\ \text{eV/°K}.$$

At room temperature, the direct gap extrapolates at 3.062 eV.

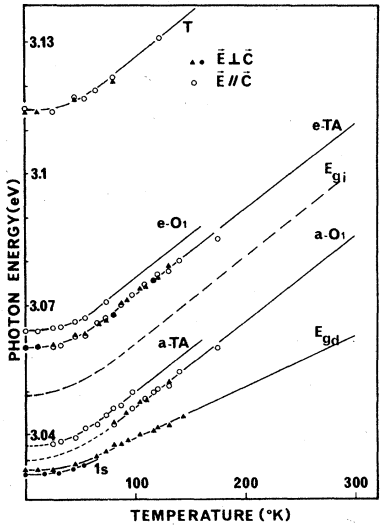

FIG. 3. Temperature dependence of the absorption components. The dashed line corresponds to the excitonic energy gap.

IV. DISCUSSION

All experimental results discussed earlier show that the fundamental absorption edge of TiO_2 is dependent on two mechanisms. The corresponding transitions are called E_{gi} and E_{gd}. They differ essentially with regard to the selection rules: E_{gi} is allowed in both polarizations while E_{gd} appears only perpendicular to $\vec{C}$. They differ also with regard to their temperature dependence: both shift to higher energy with increasing temperature but E_{gi} shifts about 10% more. We discuss separately E_{gi} in Sec. IV A and E_{gd} in Sec. IV B.

A. Fine structure of the indirect gap

The standard theory of allowed indirect transitions with creation of free excitons[9] shows that the absorption coefficient associated with an absorption or emission of a given phonon obeys the equation

$$\alpha_p(\hbar\omega) = A\left(\frac{1}{(\delta E+\hbar\Omega)^2}\ \frac{1}{e^{\hbar\Omega/kT}-1}\ (\hbar\omega - E_{gi}+\hbar\Omega)^{1/2} + \frac{1}{(\delta E-\hbar\Omega)^2}\ \frac{1}{1-e^{-\hbar\Omega/kT}} \times (\hbar\omega - E_{gi}-\hbar\Omega)^{1/2}\right), \quad (1)$$

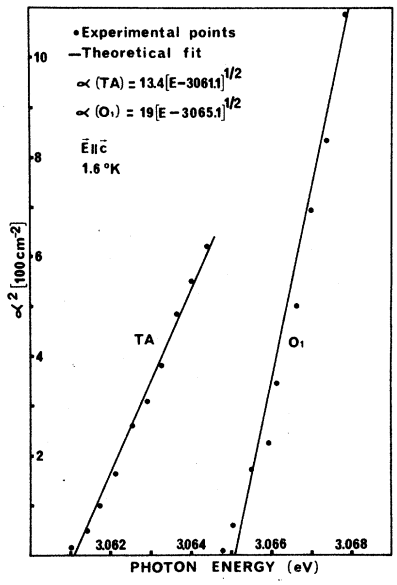

FIG. 4. Comparison of the theoretical $E^{1/2}$ dependence expected for an allowed indirect exciton with experimental data at 1.6°K.

where δE is the energy difference between the virtual state of the transition and either the initial or the final state, $\hbar\Omega$ is the phonon energy, and E_{gi} the excitonic energy gap. The absorption coefficient appears thus as a superposition of steps. Each step is associated with the threshold corresponding to an allowed excitonic transition assisted by a phonon satisfying the k-conservation rule.

In Fig. 1, we find at low temperature (1.6 °K) two steps corresponding with two different phonon emissions, O_1 (optical phonon) and TA (transverse-acoustical phonon), separated by 4 meV. The corresponding replica (absorption of phonons) are seen above 20 °K. They are also separated by 4 meV and give the two phonon energies: 11 meV for TA; 15 meV for O_1. The dashed line in Fig. 3 shows the temperature dependence of the excitonic energy gap E_{gi} obtained from the two phonon components. Within experimental error, both determinations are in good agreement and give a value $E_{gi} = 3.049$ eV at 1.6 °K.

Equation (1) suggests a characteristic linear dependence of α^2 versus energy. This is checked on Fig. 4 for the two resolved components found at 1.6 °K: α(TA) is obtained from experimental data and obeys the equation:

$$\alpha(\mathrm{TA}) = 13.4(E - 3061)^{1/2}\ \mathrm{cm}^{-1};$$

$\alpha(O_1)$ is also obtained from experimental data, subtracting the TA contribution. It obeys the equation

$$\alpha(O_1) = 19(E - 3065)^{1/2}\ \mathrm{cm}^{-1}.$$

Please note the high contribution of the second absorption edge (O_1) compared with the first threshold (TA). This large ratio of $\alpha(O_1)/\alpha(\mathrm{TA})$ (~1.4) permits us to rule out a possible misinterpretation of the data in terms of the creation of two exciton states ($n = 1$ and $n = 2$) associated with the same phonon. Indeed, in this case, we expect the first excited state ($n = 2$) to be 4 times smaller than the ground state ($n = 1$). This is in complete disagreement with the experimental value of 1.4. So we conclude that, in polarization parallel to $\vec{C}$, the fundamental edge of TiO_2 at 1.6 °K is indirect, and assisted by two phonons of energy 11 and 15 meV.

Equation (1) shows that, at a given temperature, the magnitude ratio of the absorption coefficients for the phonon emission (second term in the bracket) and phonon absorption (first term in the bracket) is

$$\frac{\alpha_e}{\alpha_a} = \left(\frac{\delta E + \hbar\Omega}{\delta E - \hbar\Omega}\right)^2 \exp\left(\frac{\hbar\Omega}{kT}\right). \qquad (2)$$

The ratio $(\delta E + \hbar\Omega)/(\delta E - \hbar\Omega)$ is only slightly temperature dependent and we expect $\ln(\alpha_e/\alpha_a)$ to be linear versus $1/T$. This has been checked for the TA phonon when α was measured at 4 meV above the two threshold energies. We show the results in Fig. 5. The straight line with an exponent of 11 meV, corresponding to the energy of the TA phonon, is in excellent agreement with the experimental points.

Now we know exactly the excitonic energy gap

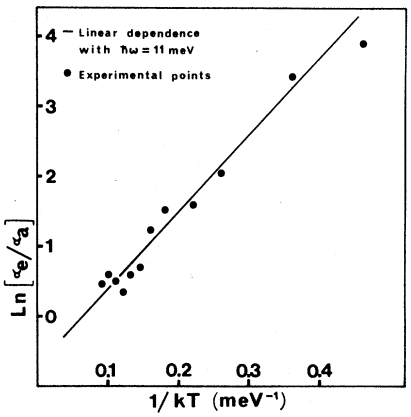

FIG. 5. Comparison of the experimental ratio α_e/α_a, corresponding with successive abosorption and emission of a given phonon, with the dependence expected from theory.

and phonon energies, we can attempt an assignment. Let us come back to the phonon dispersion data obtained by coherent inelastic scattering of thermal neutrons.[10] For clarity they are displayed in Fig. 6(a), together with the band-structure calculation of Ref. 4 [Fig. 6(b)]. A careful examination of Fig. 6(a) shows only two points in the first Brillouin zone where exist phonons of roughly 11 meV (TA mode) and 15 meV (optical mode). They are $0.2(2\pi/a)(1,1,0)$ and $0.3(2\pi/a)$ $(1,0,0)$. No such combination of energies is possible anywhere else in the Brillouin zone.

Only the first assignment is in qualitative agreement with the band-structure calculation of Ref. 4 which supports a secondary maximum of the valence band in the $[1,1,0]$ direction $[0.3(2\pi/a)$, with a Σ_4 symmetry in the single group notation]. The second possible assignment $[0.3(2\pi/a)(1,0,0)]$ would be in strong disagreement with the band-structure calculation, which shows no extremum of the valence band or of the conduction band in the $[1,0,0]$ direction [see Fig. 6(b)].

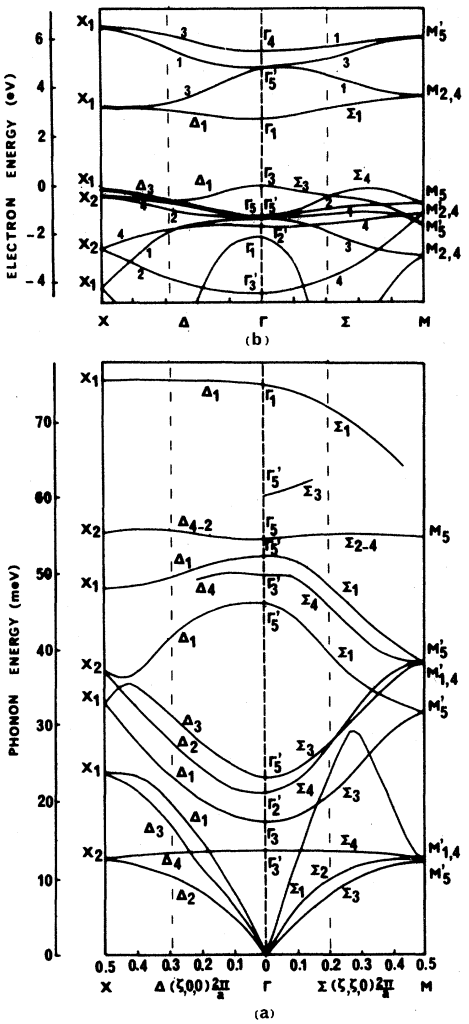

FIG. 6. (a) Phonon dispersion curves in TiO_2, after Ref. 10. The notation is given in accordance with Ref. 4. (b) Energy band structure of TiO_2 as calculated in Ref. 4.

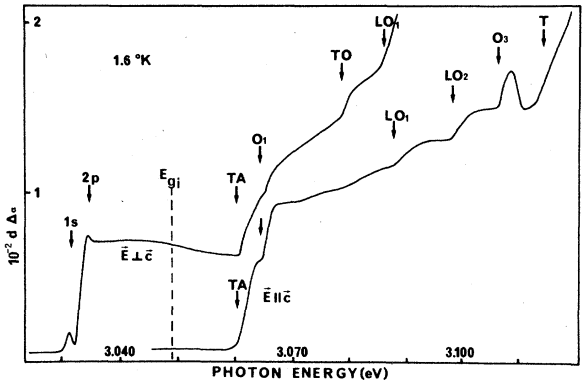

FIG. 7. High-resolution wavelength-modulated absorption data obtained at 1.6 °K on a 23-μ-thick sample. Note the narrow structures associated with the forbidden exciton ($\vec{E}\perp\vec{C}$) and the strong structure associated with the dispersionless O_3 phonon ($\vec{E}\parallel\vec{C}$).

In order to gain further support of the $[1,1,0]$ assignment we have attempted a high-resolution, wavelength-modulated investigation of the transmission data at 1.6 °K. This gives a first-order derivative of the absorption coefficient (Δa), which is shown in Fig. 7 for both polarizations.

Let us first focus on the parallel polarization. Above 3060 meV, we find several new structures listed in Table II and compare their distance in energy from the excitonic gap with the successive phonon energies at the special k point $0.2(2\pi/a)$ $(1,1,0)$. The corresponding selection rules calculated in the single group notation are illustrated

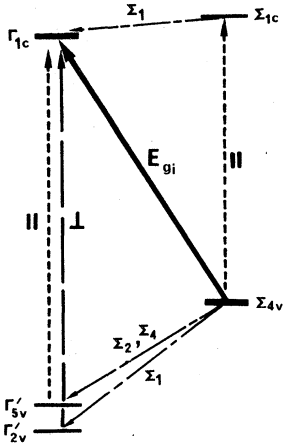

FIG. 8. Illustration of the selection rules as obtained in the single-group notation for the two special k points: $0.2(2\pi/a)$ $(1,1,0)$ and $0.3(2\pi/a)$ $(1,0,0)$. The maximum of of the valence band in the $[1,1,0]$ direction is found in the band-structure calculation. Note that it becomes Σ_5 in the double-group notation and is allowed in both polarizations.

TABLE II. Phonon energies (meV) deduced from $\Delta T/T$ spectra, compared with values obtained from the dispersion curves of Fig. 6(b). The wave vector of the phonons is $\vec{q} = 0.2(2\pi/a)(1,1,0)$.

Phonon energies from dispersion curves $\vec{q} = 0.2(2\pi/a)(1,1,0)$		Σ_3(TA) 7.9	Σ_4(TA) 9.8	$\Sigma_4(O_1)$ 13.5	Σ_3(O) 20.8	Σ_1(LA) 23.8 (weak)	Σ_4(TO) 27.2	Σ_3(TO) 27.2	$\Sigma_1(LO_1)$ 39.3	$\Sigma_4(O_2)$ 46.2	$\Sigma_1(LO_2)$ 48.7	$\Sigma_{4,2}(O_3)$ 56
Phonon energies from $\Delta T/T$ spectra	$\vec{E} \parallel \vec{C}$	Forbidden	11	15	Forbidden	...	...	Forbidden	40	...	49	58
	$\vec{E} \perp \vec{C}$	Forbidden	11	15	Forbidden	...	30	Forbidden	38	...	...	...

in Fig. 8. According to the Σ_1 symmetry of the first intermediate state in the conduction band, we find two new structures at 40 (LO_1) and 49 meV (LO_2) corresponding with the emission of the two Σ_1 optical phonons. A third Σ_1 phonon (acoustical branch) should be seen at lower energy. However, it is strongly dispersive [see Fig. 6(a)] and the corresponding density of states is expected to be very small. It is not resolved on our data. On the contrary, the dispersionless O_3 phonon of Σ_4 symmetry gives a very sharp structure. In $\vec{E} \perp \vec{C}$ polarization, the Σ_4 phonons are allowed through the Γ'_{5v} intermediate state and the corresponding structure appears well on our data at about 30 meV (TO).

B. Direct forbidden transition

In perpendicular polarization, the first structure appears at 3031 meV (1s). It is very sharp, very narrow, and characterized by a very low absorption strength ($a \sim 2$ cm^{-1}). No phonon emission assists the transition and no phonon replica could be found at lower energy in our range of investigation. It is a direct transition, but from the strength of the transition, we think it is a direct forbidden one. For example, in the continuum of absorption, 10 meV above E_{gd}, we find $\alpha \sim 100$ cm^{-1} which is too low to correspond with a direct allowed transition. The sharp structure itself appears to be a direct forbidden exciton, i.e., a second-class exciton, similar to those found in cuprous oxide.[9] This is in good agreement with the band-structure calculation which shows the first transition $\Gamma_{3v} \rightarrow \Gamma_{1c}$ is dipole forbidden.

Such forbidden transitions are characterized by vanishing matrix elements at a given critical point. However, if higher-order processes are considered, they can be found weakly allowed. For TiO_2, this is the case in polarization perpendicular to $\vec{C}$ when the excitonic interaction is properly accounted for. Let us briefly consider in more detail the creation of a direct second-class exciton. An exciton state can be regarded as the product of an envelope function $F(r_e - r_h)$, which describes the relative motion of an electron and a hole, times the Bloch function of the valence and conduction states at the critical point considered. Let Γ_c and Γ_v denote the irreducible representations of the exciton envelope function. The triple-product function constitutes a basis for the product of representation $\Gamma_c \times \Gamma_v \times \Gamma_{\text{env}}$ of the little group of $k = 0$.

The little group at Γ for TiO_2 is D_{4h}. The valence and conduction wave functions are, respectively, Γ_3 and Γ_1. The irreducible representations of the envelope functions are Γ_1 (s states),

TABLE III. Irreducible representation of electric dipole (ED), magnetic dipole (MD), and electric quadrupole (EQ) operators for TiO_2.

	ED	MD	EQ
$\vec{E}\parallel\vec{C}$	Γ_2'	Γ_5	$\Gamma_1+\Gamma_5$
$\vec{E}\perp\vec{C}$	Γ_5'	Γ_2	$\Gamma_3+\Gamma_4+\Gamma_5$

Γ_2' (p_z states), and Γ_5' (p_x and p_y states). So the exciton-state symmetries are: for the s state,

$$\Gamma_3\times\Gamma_1\times\Gamma_1=\Gamma_3;$$

for the p_z state,

$$\Gamma_3\times\Gamma_1\times\Gamma_2'=\Gamma_4';$$

and for the p_x, p_y states,

$$\Gamma_3\times\Gamma_1\times\Gamma_5'=\Gamma_5'.$$

On the other hand, the irreducible representation of electric dipole, magnetic dipole, and electric quadrupole momentum operators are given in Table III. From a comparison of exciton symmetries with creation operator symmetries, we find that (i) the creation of any kind of excitons for $\Gamma_{3v}\rightarrow\Gamma_{1c}$ is forbidden in polarization parallel to $\vec{C}$; (ii) the creation of s-type excitons is forbidden through both electric and magnetic dipole interactions and only allowed through quadrupolar electric approximation in perpendicular-to-$\vec{C}$ configuration; (iii) the creation of p-type excitons (p_x-p_y) is weakly allowed through electric dipole interaction in perpendicular-to-$\vec{C}$ configuration. All the results are in good agreement with the findings of Figs. 1 and 2 and explain the strength of the continuum absorption compared with the

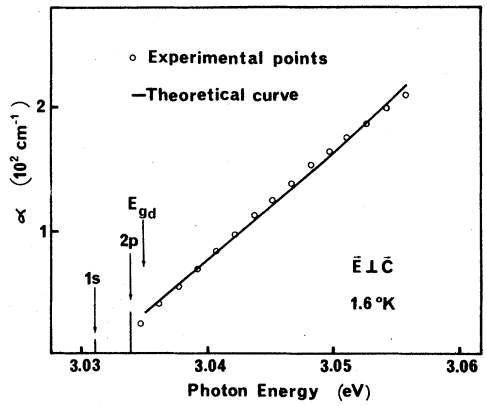

FIG. 9. Comparison of experimental data with the theoretical energy dependence of absorption expected for a direct forbidden exciton [Eq. (3)]. $C=0.7$ $meV^{-3/2}cm^{-1}$, $E=4$ meV.

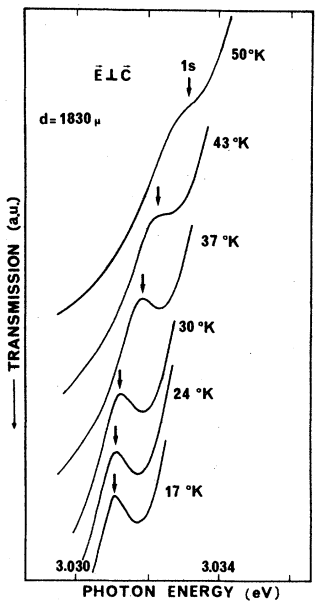

FIG. 10. High-resolution transmission data for the 1s exciton at different temperatures. ($\vec{E}\perp\vec{C}$). Note the positive temperature shift of the structure. All spectra were obtained on a 1.8-mm-thick sample.

1s excited state.

The 2p excited state is resolved on the differential spectrum of Fig. 7 at 3034 meV. Opposite to the case of first-class excitons, we find the 2p structure much more important than the 1s structure. This is in agreement with the selection rules given above. We obtain for the exciton ionization energy a very small value of about 4 meV. This value has been used to fit the direct forbidden absorption edge in light of the Elliott theory.[9] Assuming a simple hydrogenic model, the absorption strength of the continuum is

$$\alpha\sim C(\hbar\omega-E_g)^{3/2}\frac{\pi x(1+x^2)e^{\pi x}}{\sinh\pi x}, \qquad (3)$$

where $x=(E_{ex}/\hbar\omega-E_{gd})^{1/2}$.

Figure 9 shows a comparison of the experimental data with a computation of Eq. (3) assuming $E_{ex}=4$ meV. Both results are in very good agreement, which supports the very small binding energy. This is also in very good agreement with the temperature dependence found for the 1s absorption component. This is shown in Fig. 10. At helium temperature, the quadrupolar exciton is nicely resolved. It disappears rapidly when the temperature increases and becomes unresolved above 50 °K when kT becomes larger than the binding energy. The limiting value gives $kT=4$ meV.

At first sight, this value may be very surprising

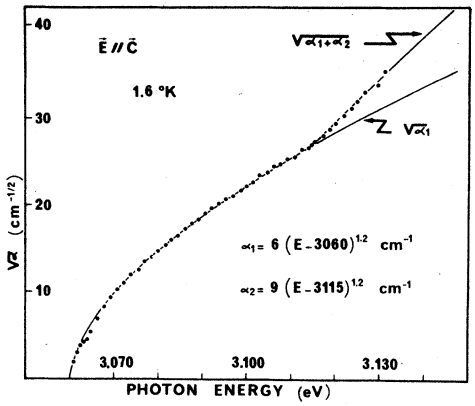

FIG. 11. Theoretical fit of the two absorption edges found in parallel polarization. The same power law $\alpha \sim (E-E_g)^{1.2}$ was used with coefficients $C_1 = 6$ cm^{-1} meV$^{-1.2}$ and $C_2 = 9$ cm^{-1} meV$^{-1.2}$. For convenience, we keep the same presentation as in Fig. 1 and plot $\sqrt{\alpha}$ vs energy.

for TiO_2, which is a wide-band-gap semiconductor; however, it is well explained by the very large values reported for the static dielectric constants[11]

$$\epsilon_{0\parallel} = 257, \quad \epsilon_{0\perp} = 111 .$$

A simple application of the standard formula,

$$E_{ex} = \frac{13.6 m^*}{\epsilon_{0\parallel}\epsilon_{0\perp}},$$

gives $m^* = 8.4 m_0$. This is in relative agreement with the electronic effective mass in TiO_2 ($m^* \sim 5m_0, 13m_0$) given by Acket and Volger.[12]

C. Higher-energy structure

A third structure, labeled T in Figs. 1 and 2, appears in both polarizations around 3114 meV at 1.6 °K.

Figure 3 shows its temperature dependence. It has the same temperature coefficient as E_{gi} but is too far away ($T - E_{gi} = 65$ meV) to be a simple phonon replica. Indeed, no strong phonon structure exists with an energy of ~65 meV in Fig. 6(a). It corresponds certainly with a new transition. On the other hand, because of the strong absorption of our thinnest sample (23 μ) in this range of energy, we have been unable to find any clear phonon replica.

In order to check whether or not it could be a direct or an indirect transition, we have attempted a simple qualitative fit. We assume α just proportional to some power of energy and fit both transitions E_{gi} and T, in polarization parallel to C. The result is shown in Fig. 11. We find that the same power law $\alpha = C(E-E_g)^{1.2}$ fit well the two sets of data. The two coefficients,

$$C_1 = 6 \text{ cm}^{-1}\text{meV}^{-1.2} \text{ and } C_2 = 9 \text{ cm}^{-1}\text{meV}^{-1.2},$$

have the same order of magnitude.

In light of the strong similarity of both transitions, we think that T is also an indirect gap transition associated with the same final state Γ_1 and a crystal field or spin-orbit structure of the valence band.

V. CONCLUSIONS

We have presented the first detailed investigation of the fundamental absorption edge of TiO_2. We have found the following.

(i) A direct forbidden transition at 3031 meV (1.6 °K). This transition is associated with the direct transition $\Gamma_{3v} \rightarrow \Gamma_{1c}$. It is strictly forbidden in polarization parallel to $\vec{C}$ and only weakly allowed, through higher-order approximation, in polarization perpendicular to $\vec{C}$. With the help of modulated transmission data, the fine structure of the exciton has been resolved and the ionization energy found is 4 meV. This is a surprisingly small value in regard of the wide band gap of TiO_2.

(ii) In both polarizations, $\vec{E} \parallel \vec{C}$ and $\vec{E} \perp \vec{C}$, an indirect transition is resolved at 3409 meV (1.6 °K) assisted by two phonons of energy 11 and 15 meV. By comparison with the phonon dispersion data, we find only two points in the Brillouin zone where the corresponding extremum of the valence band could be located $0.2(2\pi/a)(1,1,0)$ and $0.3(2\pi/a)(1,0,0)$. A detailed investigation of the wavelength modulation data supports the first assignment.

(iii) Last we have investigated a high-energy structure found at 3114 meV (1.6 °K). It corresponds with an indirect transition most probably associated with a crystal field or spin-orbit structure of the valence band.

---

*Centre associé au CNRS.

[1]M. Cardona and G. Harbeke, Phys. Rev. 137, A1467 (1965).
[2]A. Frova, P. J. Boddy, and Y. S. Chen, Phys. Rev. 157, 700 (1965).
[3]J. R. Devore, J. Opt. Soc. Am. 41, 416 (1951).
[4]N. Daude, C. Gout, and C. Jouanin, Phys. Rev. B 15, 3229 (1977).
[5]D. C. Cromemeyer, Phys. Rev. 87, 876 (1952).
[6]F. Arntz and Y. Yacoby, Phys. Rev. Lett. 17, 857 (1966).
[7]K. Vos and H. J. Krusemeyer, Solid State Commun. 15, 949 (1974).

[8]For a general discussion of modulation techniques, see, for example, M. Cardona, Solid State Phys. 11, Suppl. 1, 1969.
[9]R. J. Elliott, Phys. Rev. 108, 1384 (1957).
[10]J. G. Traylor, H. G. Smith, R. M. Nicklow, and M. K. Wilkinson, Phys. Rev. B 3, 3457 (1971).
[11]R. A. Parker, Phys. Rev. 124, 1719 (1966).
[12]G. A. Acket and J. Volger, Physica (Utr.) 32, 1680 (1962).